ISSN 1068-3356, Bulletin of the Lebedev Physics Institute, 2016, Vol. 43, No. 5, pp. 167–173. © Allerton Press, Inc., 2016.
Original Russian Text © V.S. Gorelik, A.Yu. Pyatyshev, A.S. Krylov, 2016, published in Kratkie Soobshcheniya po Fizike, 2016, Vol. 43, No. 5, pp. 26–36.

Raman Light Scattering in Sodium Nitrite Crystals

V. S. Gorelik, A. Yu. Pyatyshev, and A. S. Krylov

Lebedev Physical Institute, Russian Academy of Sciences,
Leninskii pr. 53, Moscow, 119991 Russia; e-mail: gorelik@sci.lebedev.ru

Received April 8, 2015

Abstract—Raman light scattering spectra of a ferroelectric sodium nitrite crystal is studied in the lattice mode region as the temperature is lowered from room temperature to 123 K. The existence of a Raman satellite corresponding to the soft lattice mode, i.e., transverse polar vibration responsible for the ferroelectric phase transition, is established for the first time. It is found that the intensity of the Raman scattering by the pseudo-scalar low-frequency A_2 mode exceeds the intensity of other lattice variations by an order of magnitude.

DOI: 10.3103/S1068335616050043

Keywords: sodium nitrite, Raman scattering, spectrum, polar mode, polariton, ferroelectric, dispersion curves.

Ferroelectric crystals ($BaTiO_3$, KH_2PO_4, $(NH_4)_2BeF_4$, and others) find wide application in electric and electro-optic devices (capacitors, modulators, memory cells [1, 2]). Of great importance is ferroelectric ceramics used for developing electromechanical and mechanoelectrical converters in a wide frequency range.

Among a large number of materials of this type, sodium nitrite ($NaNO_2$) is one of the simplest ferroelectric crystals in structure. At a temperature of 160 °C, the ferroelectric non-centrosymmetric-to-centrosymmetric phase transition occurs in $NaNO_2$ crystals [3]. At room temperature, sodium nitrite in the ferroelectric phase is characterized by C_{2v}^{20} (Im2m) space group. It was found that the sodium nitrite crystal structure above the Curie point corresponds to D_{2h}^{25} space group (Immm). At a temperature of 26 °C, the unit cell parameters are as follows: $a = 0.539$ nm, $b = 0.558$ nm, and c = 0.357 nm [4–6]. At a temperature of 205 °C, $a = 0.533$ nm, $b = 0.568$ nm, and $c = 0.369$ nm [4–6]. In [7, 8], it is reported on the experimental results on generation of the second optical harmonic localized in a thin surface layer of photonic crystals doped with sodium nitrite. In [9], radio-frequency radiation during phase transitions in sodium nitrite is analyzed.

The theory [5, 6, 10] predicts that an increase in the static permittivity near to the ferroelectric phase transition point is caused by the so-called soft mode in the vibrational spectrum, i.e., the transverse polar vibration totally symmetric in the pyroelectric phase.

Infrared spectra of the $NaNO_2$ crystal were studied in [11–16]. In these studies, the reflectance spectra were recorded in the frequency range of 40–600 cm^{-1} in the temperature range from 293 to 503 K. In [12, 13], reflectance spectra were analyzed using the classical oscillator model, and the temperature dependence of the parameters of transverse optical (TO) vibrations were obtained.

Raman scattering (RS) spectra of sodium nitrite crystals were studied in [17–23], where the effect of heating (in the range of 300–500 K) on the Raman spectrum was studied [17, 18]. In [19], Raman spectra of a single crystal were studied at temperatures of 77 and 294 K, and spectral bands were attributed to vibration types. It should be noted that no polar soft mode responsible for the ferroelectric phase transition was revealed in Raman spectra of sodium nitrite until now.

The objective of this work was to analyze the complete RS spectrum of the sodium nitrite crystal at various temperatures and to detect the soft mode in the spectra, predicted by the theory for ferroelectric crystals, and to study the pseudo-scalar mode appearing in the vibrational spectrum of sodium nitrite.

The block diagram of the experimental setup for exciting and recording RS spectra is shown in Fig. 1. An argon laser (1) (Spectra Physics Stabilite 2017) with a wavelength of 514.5 nm and a power of 15 mW is used as an exciting radiation source. After passing the deflecting mirror (2), laser

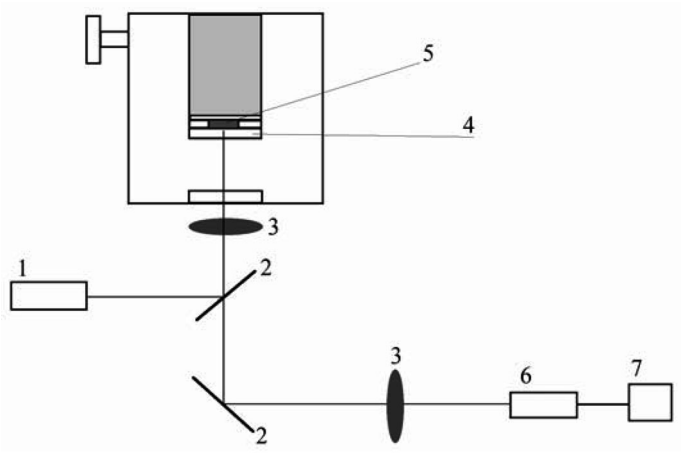

Fig. 1. Schematic diagram of the experimental setup: (1) laser, (2) mirrors, (3) objective, (4) glass substrate, (5) material under study, (6) T64000 triple monochromator, and (7) computer.

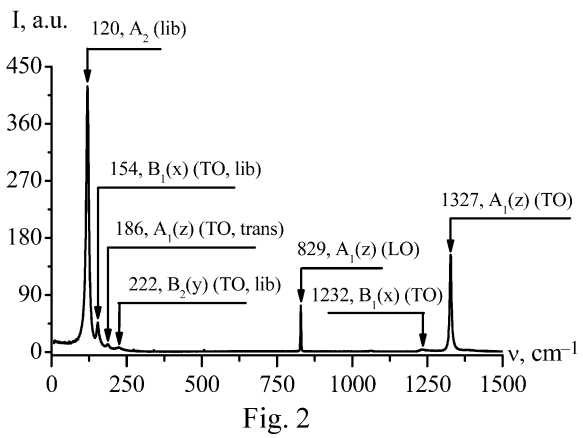

Fig. 2

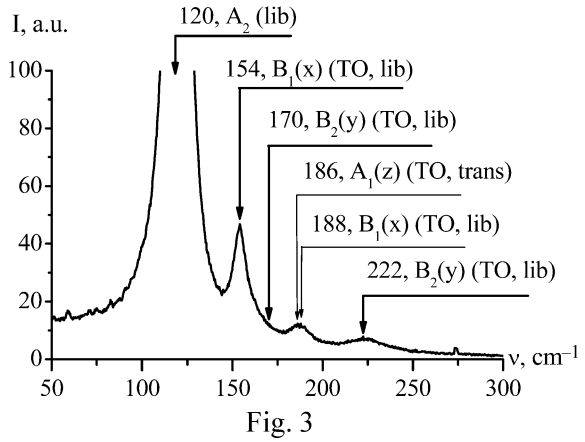

Fig. 3

Fig. 2. Raman spectrum of sodium nitrite, measured at room temperature in the frequency range from 0 to 1500 cm^{-1}.

Fig. 3. Low-frequency spectral region of sodium nitrite RS.

radiation was focused on sample (5) using microobjective (3). A 50-fold microobjective ($f = 0.8$ mm) with a numerical aperture of 0.75 was used. The sodium nitrite powder sample under study was clamped between transparent glass (4) and a liquid nitrogen container.

Scattered radiation was recorded using mirror (2) and objective (3). Raman spectra were measured using a Horiba Jobin Yvon T64000 triple monochromator (6). As a radiation detector, a CCD array was used, whose signal was sent to computer (7). The spectral resolution was 1 cm^{-1}; diffraction gratings of 1800 lines/mm were used; the entrance slit width was 0.1 mm.

Figure 2 shows the complete spectrum (in the region of lattice and intramolecular modes) of RS of sodium nitrite polycrystals, measured at room temperature in the frequency range from 0 to 1500 cm^{-1}. We can see that this spectrum consists of a portion corresponding to lattice vibrations and a portion corresponding to intramolecular vibrations. Figure 3 shows the spectral region corresponding to lattice vibrations. Arrows indicate the positions of corresponding intensity maxima; the vibration frequencies, corresponding symmetry types, and vibration attribution to the translational (trans) or librational (lib) types are also given.

Figure 4 shows the portion of the RS spectrum of lattice vibrations of sodium nitrite, measured at a temperature of 123 K in the frequency range from 0 to 300 cm^{-1}. As the crystal temperature is lowered, RS satellites in the region of lattice modes become narrower; furthermore, additional bands are detected (see Figs. 2 and 3).

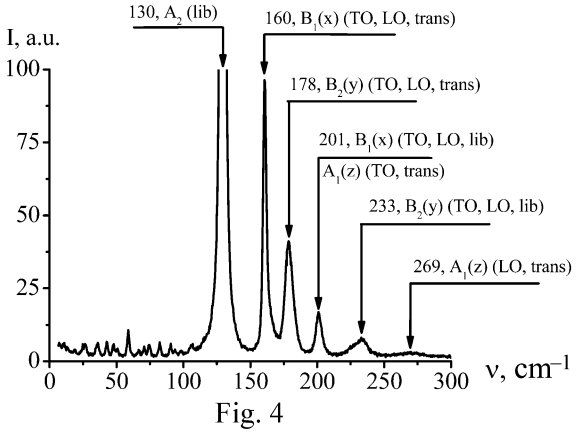

Fig. 4

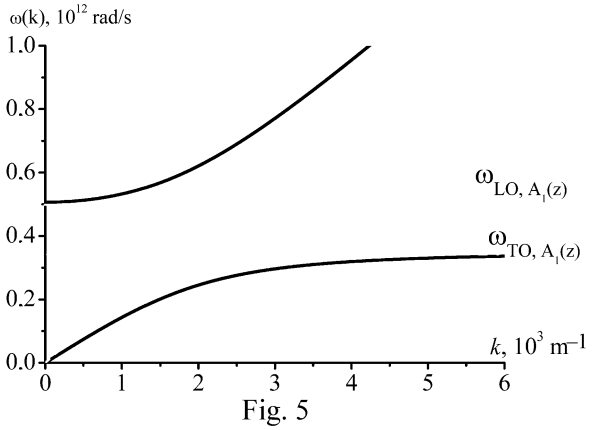

Fig. 5

Fig. 4. The portion of sodium nitrite RS spectrum, measured at a temperature of 123 K in the range from 0 to 300 cm^{-1}.

Fig. 5. Polariton curves for the mode $A_1(z)$ at room temperature.

As seen in Fig. 4, at a temperature of 123 K, the RS spectrum contains a low-frequency mode at 130 cm^{-1}, whose intensity significantly exceeds the intensities of other lattice modes. A band with an intensity maximum frequency of 269 cm^{-1}, which is absent at room temperature, is also observed.

It follows from the group-theory analysis of the sodium nitrite crystal that the spectrum of optical vibrations contains the following vibration types [24]:

$$T_{\text{opt}} = [A_1(z) + B_1(x) + B_2(y)] + [A_2 + B_1(x) + B_2(y)]+$$

$$+[A_1(z) + A_1(z) + B_1(x)]. \quad (1)$$

The first bracket corresponds to translational (trans) lattice modes (translational oscillations of the NO_2 group with respect to sodium ions); the second bracket corresponds to librations (lib) of the NO_2 group with respect to three axes; the third bracket corresponds to intramolecular (internal) vibrations of the NO_2 group. Here we note that the $A_1(z)$, $B_1(x)$, and $B_2(y)$ polar modes should appear in RS spectra as doublets, i.e., both the transverse (TO) and longitudinal (LO) components.

Table 1. Literature data on IR reflectance and RS spectra for sodium nitrite

	IR				RS						Type
	[11]		[12]		[17]		[18]		[22, 23]		
	TO	LO	TO	LO	TO	LO	TO	LO	TO	LO	
$A_1(z)$	194	269	187	–	–	–	–	–	–	–	Transla-
$B_1(x)$	157	163	151	–	153	–	154	165	158	–	tional
$B_2(y)$	149	193	146	–	–	–	150	201	–	–	
A_2	–		–		119		120		117		Libra-
$B_1(x)$	188	250	181	–	177	–	184.5	236	191	–	tional
$B_2(y)$	223	261	232	–	220	–	228	254	223	–	
$A_1(z)$	826	829	825	–	825	–	828	829	830	–	Internal
$A_1(z)$	1323	1336	1321	–	1327	–	1326	1328	1323	–	
$B_1(x)$	1235	1368	1227	–	1280	–	1225	1356	1230	–	

Table 1 lists the literature data on symmetry types and vibration types obtained previously by analyzing infrared (IR) reflectance and Raman scattering spectra for sodium nitrite crystals.

Table 2. Vibration frequencies and their attribution to symmetry types in the Raman spectrum of sodium nitrite, recorded at room temperature

Frequency, cm^{-1}	Vibration symmetry type	Phonon type	Vibration type	Type
186	$A_1(z)$	TO	Translational	Lattice
154	$B_1(x)$	TO		
170	$B_2(y)$	TO		
120	A_2		Librational	
188	$B_1(x)$	TO		
222	$B_2(y)$	TO		
829	$A_1(z)$	LO	Symmetric deformation vibration	Internal
1327	$A_1(z)$	TO	Symmetric stretching vibration	
1232	$B_1(x)$	TO	Asymmetric stretching vibration	

Table 3. Vibration frequencies and their attribution to symmetry types in the Raman spectrum of sodium nitrite, measured at temperature $T = 123$ K

Frequency, cm^{-1}	Vibration symmetry type	Phonon type	Vibration type
130	A_2		Librational
160	$B_1(x)$	TO, LO	Translational
178	$B_2(y)$	TO, LO	
201	$B_1(x)$	TO, LO	Librational
233	$B_2(y)$	TO, LO	
269	$A_1(z)$	LO	Translational

Table 2 lists the frequencies of maxima in RS spectra, observed in the present study in $NaNO_2$ polycrystals at room temperature. In contrast to the literature data (see Table 1), we detected (Figs. 2 and 3) the $A_1(z)$ lattice mode with a frequency of 186 cm^{-1} in the RS spectra, which corresponds to translational polar transverse vibration responsible for the ferroelectric phase transition. Furthermore, RS satellites are detected at room temperature, whose frequencies are in good agreement with the literature data.

Table 3 lists the measured frequencies of maxima in the low-frequency RS spectrum of sodium nitrite at $T = 123$ K.

A comparison of Figs. 2–4 and Tables 2 and 3 shows frequency shifts of RS lines to higher values as the temperature is lowered from room temperature to 123 K. Figure 4 shows the band related to the

$A_1(z)$ longitudinal (LO) mode corresponding to sodium oscillations with respect to the NO_2 group, which causes a change in the dipole moment of the primitive cell. The frequency of the transverse vibration of this type appears close to the $B_1(x)(TO)$ mode frequency of 201 cm^{-1} (see Fig. 4). This is consistent with the results of the study [11, 12] of infrared reflectance spectra, according to which the values $v(A_1, TO) = 194$ cm^{-1} and $v(A_1, LO) = 269$ cm^{-1} were obtained. We note that in the case at hand, the soft mode corresponding to the $A_1(z)(TO)$ type appears overdamped far from the ferroelectric phase transition point. This is caused by the NO_2 group reorientation about the x axis, corresponding to dephasing of the $A_1(z)(TO)$ mode. As a result, as the temperature increases, this mode transforms to a relaxor and takes the form of a broadband central peak characteristic of relaxation processes. Table 4 lists the characteristics of the soft mode of sodium nitrite, determined far from the ferroelectric transition point and the corresponding high-frequency and static permittivities.

Table 4. Parameters of polaritons for A_1 mode at room temperature

Mode	$v(TO, A_1(z))$, cm^{-1}	$v(LO, A_1(z))$, cm^{-1}	$\varepsilon_{\infty z}$ [11]	ε_{0z} [12]
$A_1(z)$	186	269	1.9	3.51

According to the known Lyddane–Sachs–Teller relation [25] for the $A_1(z)$ soft mode responsible for the ferroelectric phase transition, the ratio

$$\frac{\varepsilon_{0z}}{\varepsilon_{\infty z}} = \frac{\omega^2_{(LO,A_1(z))}}{\omega^2_{(TO,A_1(z))}} \tag{2}$$

should take place (without regard to the contribution of internal vibrations).

Substituting the values from Table 4 into ratio (2), we come to the conclusion that the Lyddane–Sachs–Teller relation is in satisfactory agreement with the performed experiments on RS spectra and the literature data on IR spectroscopy.

Based on the obtained characteristics of the soft mode, we can construct the dispersion relation for corresponding polariton curves defined by the known relation

$$\omega^2 = \frac{c_0^2 k^2}{\varepsilon_z(\omega)}, \tag{3}$$

where c_0 is the speed of light in vacuum and $\varepsilon_z(\omega)$ is the corresponding permittivity

$$\varepsilon_z(\omega) = \varepsilon_{\infty z} \cdot \frac{\omega^2_{LO,A_1(z)} - \omega^2}{\omega^2_{TO,A_1(z)} - \omega^2}. \tag{4}$$

Substituting Eq. (4) into (3), we obtain the equation of dispersion curves of polaritons,

$$\omega^4 - \omega^2 \cdot \frac{\omega^2_{LO,A_1(z)}\varepsilon_{\infty z} + c_0^2 k^2}{\varepsilon_{\infty z}} + \frac{\omega^2_{TO,A_1(z)} c_0^2 k^2}{\varepsilon_{\infty z}} = 0. \tag{5}$$

As a result, we obtain the solution for two polariton branches,

$$\omega^2_{\pm}(k) = \frac{\omega^2_{LO,A_1(z)} + c^2 k^2}{2} \left(1 \pm \sqrt{1 - \frac{4\omega^2_{TO,A_1(z)} c^2 k^2}{\left(\omega^2_{LO,A_1(z)} + c^2 k^2\right)^2}} \right). \tag{6}$$

Here $c^2 = \frac{c_0^2}{\varepsilon_{\infty z}}$, $\omega_{LO,A_1(z)} = 2\pi c_0 v(LO, A_1(z))$, and $\omega_{TO,A_1(z)} = 2\pi c_0 v(TO, A_1(z))$. The parameters $v(TO, A_1(z))$, $v(LO, A_1(z))$ and $\varepsilon_{\infty z}$ are given in Table 4. Figure 5 shows the results of the calculation of the polariton curves for the $A_1(z)$ polar mode in sodium nitrite. There are given the values of $\omega_{TO,A_1(z)}$, $\omega_{LO,A_1(z)}$ and the dispersion relation $\omega = \frac{c_0 k}{\sqrt{\varepsilon_{\infty z}}}$ (dashed lines).

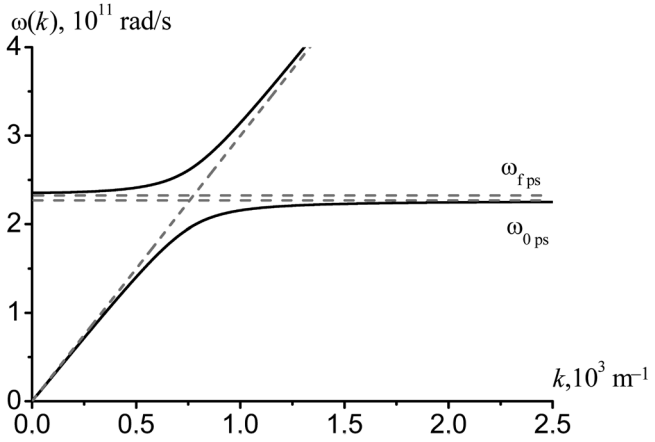

Fig. 6. Dispersion curves of axion branches in sodium nitrite.

According to the table of irreducible group C_{2V} characters [26], librational lattice vibrations such as A_2 are pseudo-scalar. According to the theoretical concepts developed in [27–34], pseudo-scalar waves corresponding to particles called the axions exist in vacuum along with electromagnetic waves. The resonant interaction of axions with pseudo-scalar phonons in a dielectric medium leads to the formation of hybrid quasiparticles, i.e., axinons [35] similar to polaritons. In [35], the dispersion relation for axinons was derived in the form

$$\omega_{\pm}^2(k) = \frac{(\omega_{f\,\mathrm{ps}}^2 + \omega_a^2 + c_0^2k^2)}{2} \cdot \left(1 \pm \sqrt{1 - \frac{4 \cdot (\omega_{0\,ps}^2 \cdot \omega_a^2 + \omega_{0\,ps}^2 c_0^2 k^2)}{(\omega_{f\,ps}^2 + \omega_a^2 + c_0^2k^2)^2}}\right). \tag{7}$$

Here $\omega_a = 2\pi c_0 v_a$, $\omega_{0\,ps} = 2\pi c_0 v_{0\,ps}$ and $\omega_{f\,ps} = 2\pi c_0 v_{f\,ps}$ are the frequencies of axions in vacuum, phonons, and hybrid mode. Let us take the following values: $v_{f\,ps} = 125$ cm^{-1}, $v_{0\,ps} = 120$ cm^{-1} (Table 2), $v_a = 1$ cm^{-1} [36, 37]. Figure 6 shows the dispersion curves of axinons in sodium nitrite, calculated by Eq. (7). In this figure, dashed lines are the values of $\omega_{f\,ps}$, $\omega_{0\,ps}$ and the photon dispersion relation in vacuum.

We can see in Fig. 6 that the branch "anticrossing" is implemented in the crossover region of the axion branch and the dispersion branch of the pseudo-scalar mode of sodium nitrite, which indicates hybridization of axions with phonons in this frequency region.

Thus, the existence of the transverse polar $A_1(z)$-type (soft) mode responsible for the ferroelectric phase transition in the sodium nitrite crystal in the RS spectrum was established for the first time. It became possible to detect it only far from the ferroelectric phase transition point. Polariton curves for the $A_1(z)$ soft mode at room temperature were constructed. As the temperature increases, this mode becomes overdamped and can appear only as a central peak. The complete Raman scattering spectrum in sodium nitrite polycrystals was measured and studied. The RS satellites and vibrations predicted by the group-theory analysis were attributed. It was found that the intensity of the low-frequency A_2 pseudo-scalar mode almost ten times exceeds the intensity of other lattice vibrations. The feasibility of hybridization of pseudo-scalar phonons with axions was discussed. The dispersion curves corresponding to hybridization of axions and pseudo-scalar phonons were constructed. The established features for polar modes and the pseudo-scalar mode in non-centrosymmetric sodium nitrite can be applied to implement parametric processes with emission in the terahertz spectral region.

ACKNOWLEDGMENTS

This study was supported by the Russian Foundation for Basic Research, projects nos. 12-02-00491, 13-02-00449, 13-02-90420, 14-02-00190.

REFERENCES

1. P. Ravindran, A. Delin, B. Johansson, O. Eriksson, Phys. Rev. B **59**, 1776 (1999).
2. J. Köhler and D. Schmid, J. Phys.: Condens. Matter **8**, 115 (1996).
3. B. Strijk, C. H. Mac Gillavry, Recueil des Travaux Chimiques des Pays-Bas **62**, 705 (1943).
4. R. W. G. Wyckoff, *Crystal Structures - Volume 2: Inorganic Compounds RXn, RnMX2, RnMX3* (Interscience, New York, 1964).
5. F. Jona and G. Shirane, *Ferroelectric Crystals* (Pergamon, Oxford—London—New York—Paris, 1962).
6. G. A. Smolenskii, V. A. Bokov, V. A. Isupov, et al., *Ferroelectrics and Antiferroelectrics* (Nauka, Leningrad, 1971) [in Russian].
7. Yu. P. Voinov, V. S. Gorelik, K. I. Zaitsev, et al., Fiz. Tverd. Tela **57**, 443 (2015) [Phys. Solid State **57**, 453 (2015)].
8. K. I. Zaitsev and S. O. Yurchenko, Appl. Phys. Lett. **105**, 051902 (2014).
9. P. F. Zilberman and P. A. Savintsev, Pisma Zh. Tekh. Fiz. **14**, 145 (1988).
10. V. L. Ginzburg, Usp. Fiz. Nauk **38**, 490 (1949).
11. J. D. Axe, Phys. Rev. **167**, 573 (1968).
12. M. K. Barnoski and J. M. Ballantyne, Phys. Rev. **174**, 946 (1968).
13. K. Suzuki, S. Sawada, F. Sugawara, and T. Nakamura, J. Phys. Soc. Japan **26**, 1199 (1969).
14. H. Vogt and H. Happ, Phys. Status Solidi **16**, 711 (1966).
15. F. Brehat and B. Wyncke, J. Phys. C: Sol. State Phys. **18**, 1705 (1985).
16. B. Wyncke, F. Brehat, M. El Sherif, and G V. Kozlov, Phys. Status Solidi (b) **125**, 493 (1984).
17. E. V. Chisler and M. S. Shur, Phys. Status Solidi (b) **17**, 163 (1966).
18. C. M. Hartwig, E. Wiener-Avnear, and S. P. S. Porto, Phys. Rev. B **5**, 79 (1972).
19. C. K. Asawa and M. K. Barnoski, Phys. Rev. B **2**, 205 (1972).
20. C. W. von der Lieth and H. H. Eysel, J. Raman Spectrosc. **13**, 120 (1982).
21. H. H. Eysel, C. W. von der Lieth, G. Bertsch and M. H. Brooker, Mol. Phys. **44**, 395 (1981).
22. M. Tsuboi, M. Terada, T. Kajiura, Bull. Chem. Soc. Japan **41**, 2545 (1968).
23. M. Tsuboi, M. Terada, T. Kajiura, Bull. Chem. Soc. Japan **42**, 1871 (1969).
24. G. Ya. Lyubarskii, *Group Theory and its Application in Physics* (Gos. Izd. Fizmatlit, Moscow, 1958) [in Russian].
25. R. H. Lyddane, R. G. Sachs, and E. Teller, Phys. Rev. **59**, 673 (1941).
26. L. D. Landau and E. M. Lifshitz, *Theoretical Physics, Vol. 3, Quantum Mechanics* (Nauka, Moscow, 2002; Pergamon Press, New York, 1959).
27. L. B. Okun, Zh. Eksp. Teor. Fiz. **83**, 892 (1982).
28. K. van Bibber, N. R. Dagdeviren, S. E. Koonin, et al., Phys. Rev. Lett. **59**, 759 (1987).
29. L. D. Duffy, P. Sikivie, D. B. Tanner, et al., Phys. Rev. D **74**, 012006 (2006).
30. P. Sikivie, D. B. Tanner and K. van Bibber, Phys. Rev. Lett. **98**, 172002 (2007).
31. A. Afanasev, O. K. Baker, K. B. Beard, et al., Phys. Rev. Lett. **101**, 120401 (2008).
32. S. Hoffmann, Phys. Lett. B **193**, 117 (1987).
33. R. Cameron, G. Cantatore, A. C. Melissinos, et al., Phys. Rev. D **47**, 3707 (1993).
34. G. Ruoso, R. Cameron, G. Cantatore, et al., Z. Phys. C: Part. Fields **56**, 505 (1991).
35. V. S. Gorelik, Kratkie Soobshcheniya po Fizike FIAN **42**(2), 40 (2015) [Bulletin of the Lebedev Physics Institute **42**, 55 (2015)].
36. C. Beck, Phys. Rev. Lett. **111**, 231801 (2013).
37. C. Hoffmann, F. Lefloch and M. Sanquer, Phys. Rev. B **70**, 180503 (2004).